International Journal of Mechanical and Production Engineering Research and Development (IJMPERD)
ISSN(P): 2249-6890; ISSN(E): 2249-8001
Vol. 8, Issue 5, Oct 2018, 417-426

THE MULTI-RESPONSE OPTIMIZATION OF MACHINING PARAMETERS IN THE ULTRASONIC ASSISTED DEEP-HOLE DRILLING USING GREY-BASED TAGUCHI METHOD

NGOC-HUNG CHU[1] & VAN-DU NGUYEN[2]

[1]*International Training Faculty, Thai Nguyen University of Technology, Viet Nam*

[2]*Mechanical Engineering Faculty, Thai Nguyen University of Technology, Viet Nam*

ABSTRACT

This paper presents a practical approach for the multiple response optimizations of operational parameters in the ultrasonic assisted drilling of deep holes. Applying the Taguchi design of experiments, a plan of 27 drilling tests on 6061 aluminium alloy with the depth-to-diameter ratio of 10 was conducted. The responses of cutting force and torque, maximum force and torque, including the chip-evacuation parts which appeared when drilling deep holes, were chosen to be optimized. Three significant drilling parameters, named vibration amplitude, feeding rate and cutting speed were found to have the most significant effects on the output responses. Based on the grey relational grade analysis and analysis of variance technique, optimum levels as well as the percentage contribution of such parameters were identified. Confirmation test was conducted to validate the test result. Experimental results showed that the multi-response optimization problem in ultrasonic assisted the deep hole drilling can be effectively addressed through the combination of Taguchi design and Grey relational analysis.

KEYWORDS: Deep Holes, Ultrasonic Assisted Drilling, Drilling Torque, Drilling Force, Grey-Based Taguchi & ANOVA

Received: Aug 04, 2018; **Accepted:** Aug 24, 2018; **Published:** Sep 22, 2018; **Paper Id.:** IJMPERDOCT201847

Original Article

1. INTRODUCTION

Drilling is one of the major mechanical machining processes, as about one-third of all manufacturing operations (Liu et al., 2000). Aluminium alloys have been widely used in applications where materials with high strength-to-weight ratio are required, such as in the rapidly growing automobile and aerospace industries. Emerging trend of dry cutting, an environmentally friendly machining technique, has also given a real challenge in drilling aluminium alloys (Roy et al., 2009). During the dry drilling process of aluminium alloys, long and ductile chips, especially in deep holes, tend to bend and coil and thus cause packing of the drill flutes, interferes with chip ejection (Drozda, 1983).

In deep hole drilling, where the aspect ratio increase further to more than about three to four times of twist drills, the torque increase exponentially (Arzur-Bomont et al., 2010), (Ke and Stephenson, 2006), (Mellingeret al., 2002), (Hanet al., 2018). As the drilling depth increases, an increased amount of chips would fill up the flutes, leading to the chip-clogging, i.e. the jamming of chips inside the flute. The addition of chip evacuation torque results in excessive torsional stress, and once the maximum torsional strength of the drill is reached, drill breakage

would occur (Mellinger et al., 2002), (Ravisubramanian & Shunmugam, 2017), (Furnesset al., 1996).

The Ultrasonic Assisted Drilling (UAD) has recently been investigated as a new, innovative and effective machining method. Compared to Conventional Drilling (CD), there have been shown significant reduction of thrust force (Aminiet al., 2013; Azghandiet al., 2016; Chang et al., 2009; Li et al., 2015, 2016), improvements in built-up edge (Amini et al., 2013; Baraniet al., 2014), burr size (Amini et al., 2013; Chang & Bone, 2010), tool life (Chang et al., 2009) and hole oversize (Amini et al., 2013)… which can be taken from Ultrasonic Assisted Drilling (UAD). A significant reduction of drilling torque of 50% when applying UAD for aluminium has been found in the study of Neuge Bauer and Stoll (Neugebauer & Stoll, 2004). However, drilling investigations have been implemented for shallow holes, where the aspect ratio L/D was only ranged from 2 to 4, while in many applications the depth of required holes are ten or more times of the hole diameter (Baghlaniet al., 2013). The effectiveness of UAD regarding to the reduction of chip evacuation torque has been found in a recent study of Chu and Nguyen (Ngoc-Hung Chu, 2018).

Taguchi technique is one of the most powerful tools in experiment design, used to select proper process parameters in machining. Mohan et al., (Mohanet al., 2005), employed Taguchi technique to scrutinize the effect of process parameters on cutting force and torque during drilling of glass-fiber polyester reinforced composite. Optimization of the tool parameters in ultrasonic vibration assisted drilling was made by using Taguchi method (Rakesh, 2016).Recently, a complementary approach using grey relational analysis (GRA)(Deng, 1989)combined with Taguchi design, shortly named as Taguchi-Grey Relational Analysis (TGRA), has been found to be effective for multi-responses optimization process. TGRA was applied in the optimization of the turning aluminium Alloy process (Jayaraman & Kumar, 2014). Rupesh et al. investigated the optimization of multiple quality characteristics in bone drilling using TGRA (Pandey and Panda, 2015). Other fields of applications have been found in drilling Medium Density Fiber Board (MDF)(Akhil et al., 2017), drilling hybrid aluminium metal matrix composites(Rajmohan et al., 2012) or bone drilling (Rupesh et al., 2015). Nevertheless, multi-response, optimizing parameters in ultrasonic assisted drilling deep holes where chip evacuation forces significantly appeared have rarely been found yet. This paper presents a practical study in this field.

2. MATERIALS AND METHOD

2.1. Experimental Setup

A schematic diagram of the experimental setup is shown in Figure 1.

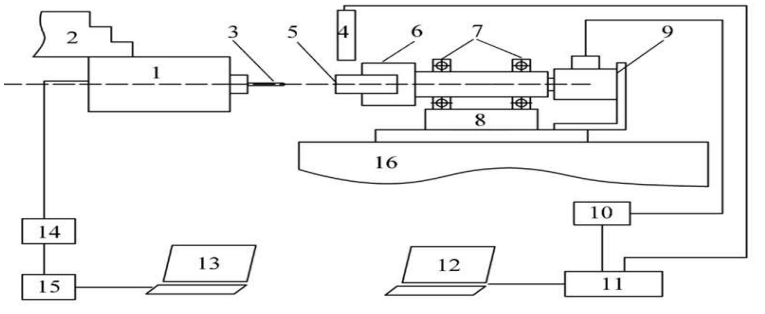

1. Rotary Vibration Actuator 2. Lathe Chuck 3. Drill Bit 4. Thermal Sensor
5. Workpiece 6. Fig 7. Bearing 8. Force Sensor
9. Torque Sensor 10. Signal Conditioner 11. DAQ
12 & 13. Computer 14. Ultrasonic Power Generator 15. Connector
16. Lathe Carriage

Figure 1: Schema of the Experimental Tests

Universal lathe machine (V-Turn 410) was used for implementing the experimental tests. Workpieces were made in the form of square bars with dimensions of 10x10x30 mm^3, made from Al6061-T6. The drilling tests were carried out using HSS twist drill bits with a diameter of 3 mm and under dry cutting conditions. The drilling torque was measured by a torque sensor model PCB-2508-03A. The axial force was measured by a force sensor Kistler 9257BA. An ultrasonic generator model MPI WG-3000 WG was used to convert 50 Hz electrical supply to high-frequency electrical impulses. The frequency range of the generator is 20 to 40 kHz and the frequency step is 1 Hz. Figure 2 presents construction of the experimental rotary UAD device.

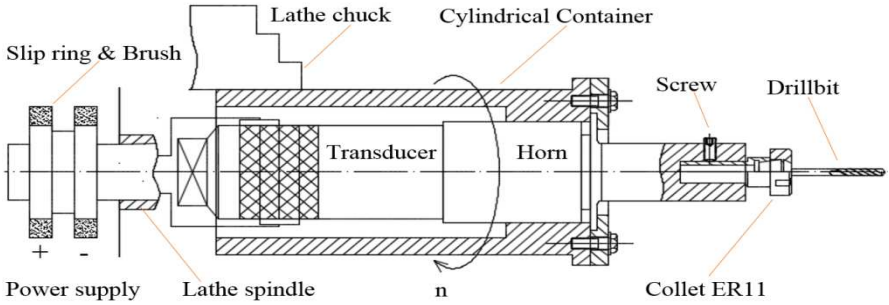

Figure 2: Structure of the Ultrasonic Vibratory Unit with Drill Bit

A commercial ultrasonic welding transducer including a proper horn and booster was fitted into a self-made steel tube and clamped at the node of the horn. The horn was modified by making a hole to put a commercial collet inside. The drilling bit was clamped inside the collet. Steady electrical impulses were supplied to the transducer via a copper brush which was positioned at the end of and rotated along with the lathe spindle. Using this arrangement, the drill bit was simultaneously received both rotation (from the lathe spindle) and longitudinal vibration (from the transducer). In this study, a commercial ultrasonic transducer working with frequency of 25 kHz and a stepped horn were selected.

2.2. Taguchi Design of Experiment and Grey-Based Optimization Process

The design of experiments was built using three cutting parameters at three levels each, thus the L27(3^3) orthogonal array is used. The investigated parameters and their levels considered in this study are shown in the Table 1.

Table 1: Input Machining Parameters and Their Levels

Parameters	Input Parameter Levels		
	Level 1	Level 2	Level 3
Speed (rpm), S	1000	1250	1500
Feed rate (mm/rev), F	0.05	0.065	0.085
Vibration amplitude (%), A	0	50	100

In Table 1, the vibration amplitude is depicted in term of percentage of output power, adjusted on the ultrasonic generator. Here 0% of amplitude means to drill without vibration, i.e. Conventional Drilling (CD). The percentage values of 50% and 100% refer to ultrasonic assisted drilling with the vibrational amplitude of the tool corresponding to 50% and 100% power applied to the ultrasonic horn.

Four objective responses of the force characteristics were chosen, including cutting force (F_{cut}), maximum force (F_{max}), cutting torque (T_{cut}) and maximum torque (T_{max}), as shown in the Figure 3. The maximum force and torque are peak values of corresponding responses during each drilling test. It would be worth noting that, cutting torque and cutting fore are usually considered as constants values in drilling (See (Mellinger et al., 2002) and (Han et al., 2018) for example).

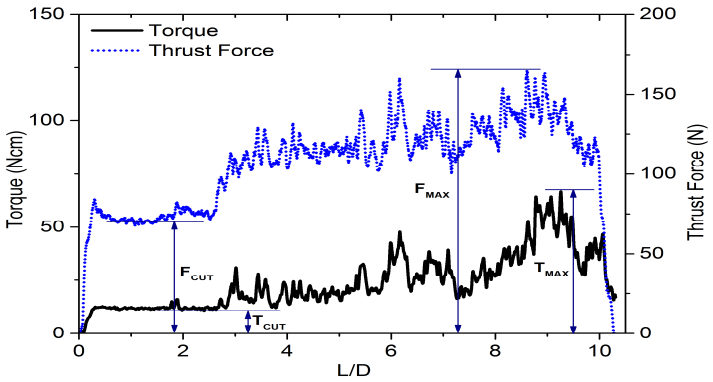

Figure 3: The Responses of Each Experimental Test

Once the normalized S/N ratio values of the responses were calculated, corresponding grey relational coefficients were carried out. Grey relational analysis was then implemented in order to find out the optimum condition. Details of calculation techniques and results are presented in the next section.

3. RESULTS AND DISCUSSIONS

The optimization process using Taguchi design and grey relational analysis and the corresponding results are depicted as below.

Step 1: Calculate the S/N Ratios

Firstly, S/N ratio for the corresponding responses was calculated. Since minimization of all characteristics is intended, the following formula for the case of Smaller-the-better was employed:

$$S/N = -10\log_{10}\left(\frac{1}{n}\sum_{i=1}^{n}\frac{1}{y_i^2}\right) \quad (1)$$

Where n is number of replications, y_{ij} is observed response value, i=1, 2, ...n; j=1, 2...k.

Table 1 depicts the input factor values and output responses of all 27 tests which were planned by Taguchi design, as well as the corresponding S/N ratios calculated using the Equation (1).

Table 1: The L_{27} Orthogonal Array, Experimental Results and Corresponding S/N Ratios

Ex. No	Input Factors			Responses				S/N Ratios			
	Speed (rpm)	Feed Rate (mm/rev)	Amplitude (%)	T_{cut} (Ncm)	T_{max} (Ncm)	F_{cut} (Ncm)	F_{max} (Ncm)	T_{cut}	T_{max}	F_{cut}	F_{max}
1	1000	0.05	0	12.09	106.99	116.37	172.98	-21.649	-40.587	-41.317	-44.760
2	1000	0.05	50	11.4	66.227	74.032	164.08	-21.138	-36.421	-37.388	-44.301
3	1000	0.05	100	9.29	35.326	69.381	145.97	-19.360	-30.962	-36.825	-43.285
4	1000	0.065	0	15.79	143.32	142.68	204.1	-23.968	-43.126	-43.087	-46.197
5	1000	0.065	50	13.98	51.23	104.46	154.92	-22.910	-34.190	-40.379	-43.802
6	1000	0.065	100	12.28	34.016	83.139	152.23	-21.784	-30.634	-38.396	-43.650
7	1000	0.085	0	22.58	115.37	188.88	269.53	-27.074	-41.242	-45.524	-48.612
8	1000	0.085	50	20.38	58.253	112.741	160.08	-26.184	-35.306	-41.042	-44.087
9	1000	0.085	100	18.65	52.459	101.02	146.71	-25.414	-34.396	-40.088	-43.329
10	1250	0.05	0	11.54	107.94	134.05	184.03	-21.244	-40.664	-42.545	-45.298
11	1250	0.05	50	6.1	35.583	91.984	153.88	-15.707	-31.025	-39.274	-43.744
12	1250	0.05	100	6.5	36.319	70.267	129.23	-16.258	-31.203	-36.935	-42.227

13	1250	0.065	0	12.46	112.65	185.61	270.55	-21.910	-41.035	-45.372	-48.645
14	1250	0.065	50	9.39	66.015	84.845	159.3	-19.453	-36.393	-38.573	-44.044
15	1250	0.065	100	10.5	42.269	76.684	161.39	-20.424	-32.520	-37.694	-44.158
16	1250	0.085	0	15.27	116.39	191.64	268.12	-23.677	-41.318	-45.650	-48.567
17	1250	0.085	50	10.53	57.548	106.17	215.35	-20.449	-35.201	-40.520	-46.663
18	1250	0.085	100	13.303	27.831	116.87	171.16	-22.479	-28.891	-41.354	-44.668
19	1500	0.05	0	13.19	127.24	131.34	286.69	-22.405	-42.092	-42.368	-49.148
20	1500	0.05	50	9.06	99.596	84.177	153.93	-19.143	-39.965	-38.504	-43.746
21	1500	0.05	100	7.4	81.069	70.919	163.8	-17.385	-38.177	-37.015	-44.286
22	1500	0.065	0	13.85	129.9	148.63	195.89	-22.829	-42.272	-43.442	-45.840
23	1500	0.065	50	12.18	58.932	80.07	168.73	-21.713	-35.407	-38.069	-44.544
24	1500	0.065	100	10.73	42.749	74.531	146.95	-20.612	-32.619	-37.447	-43.343
25	1500	0.085	0	18.58	120.7	222.49	294.92	-25.381	-41.634	-46.946	-49.394
26	1500	0.085	50	13.08	65.768	116.62	239.17	-22.332	-36.360	-41.335	-47.574
27	1500	0.085	100	12.61	57.887	116.9	197.03	-22.014	-35.252	-41.356	-45.891

Step 2: Calculate Normalized S/N Ratios and Grey Relational Coefficients

In order to prepare the data for the grey relation analysis, S/N ratios were then normalized. An appropriate value is deducted from the values in the same array to make the value approximate to 1(Jayaraman & kumar, 2014). The normalized S/N ratios were calculated using the following expression:

$$Z_{ij} = \frac{y_{ij} - min\left(y_{ij}, i = 1,2,...n\right)}{max\left(y_{ij}, i = 1,2,...n\right) - min\left(y_{ij}, i = 1,2,...n\right)} \quad (2)$$

The normalized S/N ratio values obtained were then used to calculate the grey relational coefficients by using the following formula (Jayaraman & kumar, 2014):

$$\gamma\left(y_0(k), y_i(k)\right) = \frac{\Delta min + \xi \Delta max}{\Delta_{0j}(k) + \xi \Delta max} \quad (3)$$

Where j=1,2..n; k=1,2..m; *n* is the number of experimental data items and *m*is the number of responses; $y_0(k)$is the reference sequence; $y_j(k)$is the specific comparison sequence.; Δ_{0j} is the absolute value of the difference between$y_0(k)$and $y_j(k)$; Δ_{min} and Δ_{max} are the smallest and largest values of $y_i(k)$, respectively; $\xi$is the distinguishing coefficient, $0 \leq \xi \leq 1$.

The normalized S/N ratio Values and the corresponding Grey relational coefficients are given in Table 2.

Table 2: Normalized Values of S/N Ratios and Grey Relational Coefficients

Experiments	Normalized Values of S/N Ratios				Grey Relational Coefficients				Grey Grade	Order
	T_{cut}	T_{max}	F_{cut}	F_{max}	T_{cut}	T_{max}	F_{cut}	F_{max}		
1	0.477	0.178	0.556	0.647	0.489	0.378	0.530	0.586	0.496	18
2	0.522	0.471	0.944	0.711	0.511	0.486	0.900	0.633	0.633	9
3	0.679	0.855	1.000	0.852	0.609	0.775	1.000	0.772	0.789	2
4	0.273	0.000	0.381	0.446	0.408	0.333	0.447	0.474	0.416	22
5	0.366	0.628	0.649	0.780	0.441	0.573	0.587	0.695	0.574	14
6	0.465	0.878	0.845	0.801	0.483	0.803	0.763	0.716	0.691	6
7	0.000	0.132	0.141	0.109	0.333	0.366	0.368	0.359	0.357	26
8	0.078	0.549	0.583	0.741	0.352	0.526	0.545	0.658	0.520	16
9	0.146	0.613	0.678	0.846	0.369	0.564	0.608	0.765	0.576	13
10	0.513	0.173	0.435	0.572	0.507	0.377	0.469	0.539	0.473	19
11	1.000	0.850	0.758	0.788	1.000	0.769	0.674	0.703	0.786	3
12	0.952	0.838	0.989	1.000	0.912	0.755	0.979	1.000	0.911	1

13	0.454	0.147	0.156	0.105	0.478	0.370	0.372	0.358	0.394	24
14	0.670	0.473	0.827	0.746	0.603	0.487	0.743	0.664	0.624	10
15	0.585	0.745	0.914	0.731	0.546	0.662	0.853	0.650	0.678	7
16	0.299	0.127	0.128	0.115	0.416	0.364	0.364	0.361	0.377	25
17	0.583	0.557	0.635	0.381	0.545	0.530	0.578	0.447	0.525	15
18	0.404	1.000	0.553	0.659	0.456	1.000	0.528	0.595	0.645	8
19	0.411	0.073	0.452	0.034	0.459	0.350	0.477	0.341	0.407	23
20	0.698	0.222	0.834	0.788	0.623	0.391	0.751	0.702	0.617	11
21	0.852	0.348	0.981	0.713	0.772	0.434	0.964	0.635	0.701	5
22	0.373	0.060	0.346	0.496	0.444	0.347	0.433	0.498	0.431	21
23	0.472	0.542	0.877	0.677	0.486	0.522	0.803	0.607	0.605	12
24	0.568	0.738	0.939	0.844	0.537	0.656	0.891	0.762	0.712	4
25	0.149	0.105	0.000	0.000	0.370	0.358	0.333	0.333	0.349	27
26	0.417	0.475	0.554	0.254	0.462	0.488	0.529	0.401	0.470	20
27	0.445	0.553	0.552	0.489	0.474	0.528	0.528	0.494	0.506	17

Step 3: Calculate Grey Relational Grades and Determine the Optimum Cutting Condition

Next, the grey relational grades were calculated using the following formula:

$$\overline{\gamma}_j = \frac{1}{k}\sum_{i=1}^{m}\gamma_{ij} \qquad (4)$$

Table 3 shows the grey relational grades with respect to the different input parameters, where underlined values present inputs of the optimum condition. Because the higher grey relational grade indicates the better product quality, the optimal level for each input parameter can be determined as the highest value in the investigated range, as shown in underlined values in the Table. The data were then plotted as shown in the Figure 4.

Table 3: Corresponding Grey Relational Grades of the Tests

Levels	Parameters		
	Speed, S	Feed Rate, F	Amplitude, A
1	0.5613	0.6459*	0.4109
2	0.6015*	0.5694	0.5949
3	0.5329	0.4805	0.6899*
Delta	0.0685	0.1654	0.2791
Rank	3	2	1

Note: *Optimal level of parameter. Mean value of grey relational grade: 0.565

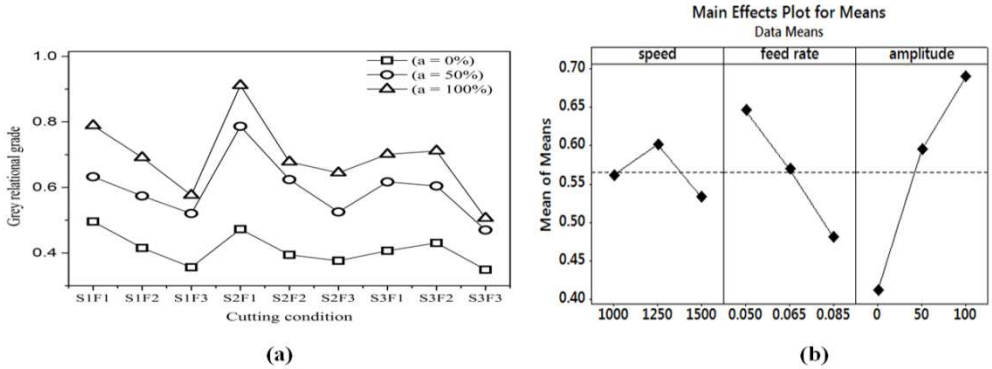

(a) (b)

Figure 4: (a) Grey Grades with Respects to Cutting Conditions and (b)Factor Effects on Grade Values

In Figure 4(a), the cutting condition S_i, F_i represents for the combination of Speed (S) and Feed (F), respectively, at level number *i* (*i*=1,2,3). As can be seen in the Figure, at each cutting condition, higher amplitude of the ultrasonic amplitude provided a higher grey grade. The both plots also show that, the highest grey grade appeared at S2F1A3, as agreed with data in Table 3.

Step 4: Perform Analysis of Variance (ANOVA)

Analysis of variance (ANOVA) is the application of a statistical method to identify the effect of individual factors. The percentage of contribution calculated from ANOVA can be used to estimate the importance of each parameter on the performance responses. The results of ANOVA and contribution of each factor are depicted in the Table 4.

As can be seen from the Table 4, the vibration amplitude has the most important effect on the responses (65%), followed by the feed rate (22%), then the speed (4%).

Table 4: ANOVA for Grey Relational Grades

Source	DF	Seq SS	Adj SS	Adj MS	F	P	Contribution (%)
Speed	2	0.02136	0.02136	0.010678	6.02	0.011	4
Feed rate	2	0.12331	0.12331	0.061653	34.76	0.000	22
Amplitude	2	0.36231	0.36231	0.181157	102.12	0.000	65
Speed*Feed rate	4	0.02097	0.02097	0.005242	2.95	0.053	4
Residual Error	16	0.02838	0.02838	0.001774			
Total	26	0.55633					

Step 5: Predict the Optimum Response

Using the optimal level of the input parameters data shown in Table 3, the estimated S/N ratio can be calculated as the following formula:

$$\hat{\eta} = \eta_m + \sum_{i=1}^{q} (\eta_i - \eta_m) \quad (5)$$

Where η_m is total mean of grey relational grade, η_i is the mean of grey relational grade at optimal level, and *q* is the number of parameters that significantly affect the performance characteristics. Substituting η_m = 0.565, q= 3 into Equation (5), we obtain:

$\hat{\eta}$ = 0.565 + (0.6899 - 0.565) + (0.6459 - 0.565) + (0.6015 - 0.565) = 0.8073

This value will be used so check with the confirmation experiment.

Step 6: Confirmation Experiment

The confirmation experiment was conducted at the optimum level of input parameters to verify the predicted result. As predicted in step 3, the optimum level of input parameters is S2F1A3, i.e. S=1250 rpm, F=0.05 mm/rev and A=100%. Confirmation experiment was implemented with those parameters. Table 5 depicts the confirmation result obtained and compared to the initial experiment S1F1A1.

Results

The confirmation experiment was conducted at the optimum level of input parameters to verify the predicted result. As predicted in step 3, the optimum level of input parameters is S2F1A3, i.e. S=1250 rpm, F=0.05 mm/rev and A=100%. Confirmation experiment was implemented with those parameters. Table 5 depicts the confirmation result obtained and compared to the initial experiment S1F1A1.

Table 5: For Initial and Optimal Machining Responses

Setting Level	Initial Data S1F1A1	Optimal Machining Parameters	
		Prediction S2F1A3	Experiment S2F1A3
T_{cut} (N.cm)	12.09	0.8073	6.5
T_{max}(N.cm)	106.99		36.319
F_{cut} (N)	116.37		70.267
F_{max}(N)	172.98		129.23
GRG	0.496		0.911
Improvement in GRG	0.104		

As it can be seen in the Table 5, each of the four considered responses appeared to be significantly smaller than that of the reference results. Compared to the predicted S/N ratio of 0.8073 as calculated by Equation (4), the confirmation experiment S/N ratio is of 0.911, more than 10% improved. Consequently, it can be said that, the Taguchi grey-based for the optimization of the multi-response problems would be a very useful tool for predicting the optimum machining condition in the ultrasonic assisted drilling of deep holes.

4. CONCLUSIONS

The optimum cutting parameters of multi-response problem in the deep hole ultrasonic assisted drilling was carried out by employing Taguchi design of experiments combined with the Grey relational analysis. The cutting torque and cutting force, the maximum torque and force, including chip-evacuation parts, were experimentally measured, collected and analysed. The following remarks can be concluded:

- The combination of Taguchi design of experiment and grey relational analysis (TGRA) would be a useful but not very complex tool for multi-objective optimization of the operational parameters in ultrasonic assisted deep hole drilling;
- It has been revealed that, ultrasonic vibration amplitude, feeding rate and cutting speed are three essential factors providing major effects on the forces and torques in the ultrasonic assisted deep hole drilling;
- The optimum condition was predicted by TGRA and verified by confirmation experiments. The results showed that TGRA would be a very promising to address the multi-response optimization problems in practical machining fields.

REFERENCES

1. *Akhil, K. T., Shunmugesh, K., Aravind, S., & Pramodkumar, M. (2017). Optimization of Drilling Characteristics using Grey Relational Analysis (GRA) in Glass Fiber Reinforced Polymer (GFRP). Materials Today: Proceedings, 4(2, Part A), 1812-1819. doi: https://doi.org/10.1016/j.matpr.2017.02.024*
2. *Amini, S., Paktinat, H., Barani, A., & Tehran, A. F. (2013). Vibration Drilling of Al2024-T6. Materials and Manufacturing Processes, 28(4), 476-480. doi: 10.1080/10426914.2012.736659*
3. *Arzur-Bomont, A., Confente, M., Schneider, E., Bomont, O., & Lescalier, C. (2010). Machinability in drilling mechanistic approach and new observer development. International Journal of Material Forming, 3(S1), 495-498. doi: 10.1007/s12289-010-0815-z*
4. *Azghandi, B. V., Kadivar, M. A., & Razfar, M. R. (2016). An Experimental Study on Cutting Forces in Ultrasonic Assisted Drilling. Procedia CIRP, 46, 563-566. doi: 10.1016/j.procir.2016.04.070*
5. *Baghlani, V., Mehbudi, P., Akbari, J., & Sohrabi, M. (2013). Ultrasonic Assisted Deep Drilling of Inconel 738LC Superalloy. Procedia CIRP, 6, 571-576. doi: 10.1016/j.procir.2013.03.096*
6. *Barani, A., Amini, S., Paktinat, H., & Fadaei Tehrani, A. (2014). Built-up edge investigation in vibration drilling of Al2024-T6. Ultrasonics, 54(5), 1300-1310. doi: 10.1016/j.ultras.2014.01.003*
7. *Chang, S. S. F., & Bone, G. M. (2010). Burr height model for vibration assisted drilling of aluminum 6061-T6. Precision Engineering, 34(3), 369-375. doi: 10.1016/j.precisioneng.2009.09.002*
8. *Chang, S. S. F., Bone, Gary M. (2009). Thrust force model for vibration-assisted drilling of aluminum 6061-T6. International Journal of Machine Tools and Manufacture, 49(14), 1070-1076. doi: 10.1016/j.ijmachtools.2009.07.011*
9. *Deng, J. L. (1989). Introduction to Grey system theory. J. Grey Syst., 1(1), 1-24.*
10. *Drozda, T. J. (1983). Tool and Manufacturing Engineers Handbook: Machining: Society of Manufacturing Engineers.*
11. *Furness, R. J., Ulsoy, A. G., & Wu, C. L. (1996). Feed, Speed, and Torque Controllers for Drilling. Journal of Engineering for Industry, 118(1), 2. doi: 10.1115/1.2803645*
12. *Han, C., Zhang, D., Luo, M., & Wu, B. (2018). Chip evacuation force modelling for deep hole drilling with twist drills. The International Journal of Advanced Manufacturing Technology. doi: 10.1007/s00170-018-2488-6*
13. *Jayaraman, P., & kumar, L. M. (2014). Multi-response Optimization of Machining Parameters of Turning AA6063 T6 Aluminium Alloy using Grey Relational Analysis in Taguchi Method. Procedia Engineering, 97, 197-204. doi: 10.1016/j.proeng.2014.12.242*
14. *Ke, F., Ni, J., & Stephenson, D. A. (2006). Chip thickening in deep-hole drilling. International Journal of Machine Tools and Manufacture, 46(12-13), 1500-1507. doi: 10.1016/j.ijmachtools.2005.09.022*
15. *Li, X., Meadows, A., Babitsky, V., & Parkin, R. (2015). Experimental analysis on autoresonant control of ultrasonically assisted drilling. Mechatronics, 29, 57-66. doi: 10.1016/j.mechatronics.2015.05.006*
16. *Li, X. F., Dong, Z. G., Kang, R. K., Wang, Y. D., Liu, J. T., & Zhang, Y. (2016). Comparison of Thrust Force in Ultrasonic Assisted Drilling and Conventional Drilling of Aluminum Alloy. Materials Science Forum, 861, 38-43. doi: 10.4028/www.scientific.net/MSF.861.38*
17. *Liu, H. S., Lee, B. Y., & Tarng, Y. S. (2000). In-process prediction of corner wear in drilling operations. Journal of Materials Processing Technology, 101(1), 152-158. doi: https://doi.org/10.1016/S0924-0136(00)00434-9*

18. *Mellinger, J. C., Burak Ozdoganlar, O., DeVor, R. E., & Kapoor, S. G. (2002). Modeling Chip-Evacuation Forces and Prediction of Chip-Clogging in Drilling. Journal of Manufacturing Science and Engineering, 124(3), 605. doi: 10.1115/1.1473146*

19. *Mohan, N. S., Ramachandra, A., & Kulkarni, S. M. (2005). Influence of process parameters on cutting force and torque during drilling of glass–fiber polyester reinforced composites. Composite Structures, 71(3-4), 407-413. doi:*

    10.1016/j.compstruct.2005.09.039

20. *Neugebauer, R., & Stoll, A. (2004). Ultrasonic application in drilling. Journal of Materials Processing Technology, 149(1-3), 633-639. doi: 10.1016/j.jmatprotec.2003.10.062*

21. *Ngoc-Hung Chu, Van-Du Nguyen (2018). A study on the reduction of chip evacuation torque in ultrasonic assisted drilling of small and deep holes. International Journal of Mechanical Engineering and Technology (IJMET), 9(6), 899-908.*

22. *Pandey, R. K., & Panda, S. S. (2015). Optimization of multiple quality characteristics in bone drilling using grey relational analysis. J Orthop, 12(1), 39-45. doi: 10.1016/j.jor.2014.06.003*

23. *Pandey, R. K., & Panda, S. S. (2015). Optimization of multiple quality characteristics in bone drilling using grey relational analysis. Journal of Orthopaedics, 12(1), 39-45. doi: https://doi.org/10.1016/j.jor.2014.06.003*

24. *Rajmohan, T., Palanikumar, K., & Kathirvel, M. (2012). Optimization of machining parameters in drilling hybrid aluminium metal matrix composites. Transactions of Nonferrous Metals Society of China, 22(6), 1286-1297. doi: 10.1016/s1003-6326(11)61317-4*

25. *Rakesh, D. D. (2016). Optimization of the tool parameters in ultrasonic vibration assisted drilling by taguchi method. International Journal of Mechanical and Production Engineering Research and Development (IJMPERD), 6(2), 1-9.*

26. *Ravisubramanian, S., & Shunmugam, M. S. (2017). Investigations into peck drilling process for large aspect ratio microholes in aluminum 6061-T6. Materials and Manufacturing Processes, 33(9), 935-942. doi: 10.1080/10426914.2017.1376076*

27. *Roy, P., Sarangi, S. K., Ghosh, A., & Chattopadhyay, A. K. (2009). Machinability study of pure aluminium and Al–12% Si alloys against uncoated and coated carbide inserts. International Journal of Refractory Metals and Hard Materials, 27(3), 535-544. doi: 10.1016/j.ijrmhm.2008.04.008*

28. *Raja, R., & Jannet, S. Experimental investigation of high speed drilling of glass fiber reinforced plastic (GFRP) composite laminates made up of different polymer matrices.*